

# MAGMA DIFFERENTIATION IN SHALLOW, THERMALLY ZONED MAGMA CHAMBERS: THE EXAMPLE OF SABATINI VOLCANIC DISTRICT (CENTRAL ITALY)

MATTEO MASOTTA

Dipartimento di Scienze della Terra, Università “La Sapienza” di Roma, Piazzale Aldo Moro 5, 00185 Roma, Italy

## INTRODUCTION

The complexity of volcanism in central Italy animated the scientific debate during the last decades. The peculiar potassium-rich magmatism of the Roman Province (Peccerillo, 2005) aimed numerous scientific contributions focused on the petrology of the various volcanic districts. Among these, the Sabatini Volcanic District (hereafter SVD) is one of the largest, being characterized by a number of explosive eruptions emplaced during the last 800 kyr that produced pyroclastic deposits cropping out in a widespread area at north of Rome (~ 1800 km<sup>2</sup>, Sottili *et al.*, 2010). During these explosive eruptions (mostly known as yellow tuffs and red tuffs), large volumes of phonolitic magmas were emplaced (an average of 10 km<sup>3</sup> dense rock equivalent of magma). The interest for these pyroclastic deposits (quarried since the ancient Roman age) promoted detailed studies, mainly on stratigraphy and geochronology (Karner *et al.*, 2001; Sottili *et al.*, 2010), whereas petrological studies are scarce. The petrological studies are, indeed, limited to lava flows and scoria cones with primitive chemical composition (*i.e.*, Cundari, 1979; Conticelli & Peccerillo, 1992; Conticelli *et al.*, 1997) that represent only a small fraction (less than 10%) of the total volume of the emplaced products.

One of the major features of SVD pyroclastic deposits is the textural variability of juvenile clasts. These deposits are commonly characterized by a transition from crystal-poor juvenile clasts at their bottom, toward crystal-rich ones at the top. In general, phonolitic volcanism offers numerous examples of pyroclastic successions showing analogue textural variations of the juvenile component, often accompanied by chemical variation of the juvenile clasts. These variations are commonly interpreted in the light of compositional variation of the erupted magma, resulting from the compositional and/or thermal layering of shallow magma chambers. However, zoning models based on compositional variations invoked for these magmatic systems, do not strictly apply in the case of SVD eruptions, given that no significant chemical variation is observed between the crystal-poor and the crystal-rich juvenile fraction. In addition to the problem of textural variations of the juvenile component, it comes up the paradox on the genesis of crystal-poor, differentiated magmas. Crystallization is intrinsic in the differentiation, but crystal fractionation may be not so obvious in a differentiated magma (*i.e.*, low contrast of densities between melt and crystal, high viscosity of the melt). Hence, mechanisms alternative to crystal settling need to be found to explain the formation of crystal-poor, differentiated magmas.

In this study, the products from large explosive eruptions of SVD were collected and investigated in detail. Phase equilibria experiments, coupled with MELTS simulations (Ghiorso & Sack, 1995), were used to constrain both differentiation and pre-eruptive conditions of the phonolitic system. Moreover, temperature gradient experiments were performed with the aim to mimic conditions occurring in a thermally zoned magma chamber and explain the observed textural variation in the deposits. Through the coupling of natural and experimental data, magmatic processes occurring in the shallow, thermally zoned magma system of SVD were modelled, addressing the problems of melt differentiation, crystal-melt separation and achievement of pre-eruptive conditions of phonolitic magmas feeding large explosive eruptions.

## GEOLOGICAL SETTING

The SVD extends over an area of ~ 1800 km<sup>2</sup> in the central part of the Roman Province and is bordered by the Tolfetano-Cerite-Manziate silicic volcanic district (6.4-1.8 Myr, De Rita *et al.*, 1993) on the west side and

by the Tiber Valley on the east side. The volcanic products interfinger to the south with the 0.56-0.35 Myr-old pyroclastic deposits of the Tuscolano-Artemisio phase (De Rita *et al.*, 1988) of the Colli Albani Volcanic District, and they are buried to the north by the 0.15 Myr-old Vico C Ignimbrite (Cioni *et al.*, 1987) from the Vico Volcanic District. The areal activity of the SVD was characterised by highly explosive, caldera-forming eruptions that produced widespread sub-plinian and plinian fall deposits. These eruptions were generally associated to weakly explosive post-caldera activity that produced lavas and scoria cones. Hydromagmatic activity dominated the most recent phases, occurring prevalently in the horst areas of the carbonate substrate (Sottili *et al.*, 2012). The SVD products cover the entire spectrum from tephrite to phonolite compositions, with minor latitic and trachytic types. However, magmas feeding large explosive eruptions are generally phonolitic in composition.

## EXPERIMENTAL METHODS AND ANALYTICAL TECHNIQUES

Phase equilibria and thermal gradient experiments were performed at the HP-HT Laboratory of Experimental Volcanology and Geophysics of Istituto Nazionale di Geofisica e Vulcanologia (INGV, Rome, Italy), using a Quickpress type non end-load piston cylinder. Further H<sub>2</sub>O-CO<sub>2</sub>-bearing phase equilibria experiments were performed at the HP Laboratory of the Department of Chemistry and Biochemistry of Arizona State University (Tempe, Arizona, USA) using the same piston cylinder device. Experiments were carried out in 19 mm, 19-25 mm and 25 mm assemblies (see Masotta *et al.*, 2012a, b for further details on these experimental procedures) in the pressure range from 200 to 300 MPa and in the temperature range from 800 to 1050 °C.

Back-scattered images of natural and experimental products were obtained at INGV using a Jeol FE-SEM 6500F equipped with an energy dispersive microanalysis system. Bulk composition of natural samples were determined by XRF analysis on glassy beads by using the Philips PW1480/10 spectrometer at Dipartimento di Scienze della Terra, Università “La Sapienza” (Rome, Italy). EMP analyses were performed both at CNR-Istituto di Geologia Ambientale e Geoingegneria (IGAG, Rome, Italy) and INGV. Compositional analyses were performed at CNR-IGAG using a CAMECA SX-50 WDS microprobe and at INGV using a Jeol-JXA8200 EDS-WDS combined electron microprobe, both equipped with five wavelength-dispersive spectrometers.

## RESULTS AND DISCUSSION

### *Natural products*

Juvenile clasts and lithic enclaves were collected from deposits of the major explosive eruptions of SVD. These deposits are commonly characterized by the occurrence of: 1) crystal-poor, white pumices at the bottom/centre of the deposits (*i.e.*, crystal-poor magma erupted in the early stage of the eruption), 2) crystal-rich, black-grey scoriae at the top of the pyroclastic deposits (*i.e.*, crystal-rich magma erupted following the crystal-poor one), and 3) lithic enclaves occurring at the top of the eruptive succession, in association with the crystal-rich scoriae.

White pumices are characterized by subaphyric texture (PI < 10%), vitrophyric groundmass (glass > 50 vol.%) and moderate vesicularity (up to 50 vol.% in thin section). They contain scarce clinopyroxene, sanidine, plagioclase and oxide phenocrysts (> 100 µm). In particular, sub-millimeter-sized, euhedral to subhedral, clinopyroxene occurs as either single phenocrysts or glomerocrysts associated with plagioclase and oxides. Sanidine is millimeter- to submillimeter-sized, round-shaped, and often glass-embayed. Very small-sized (< 30 µm) leucite typically occurs in glassy vesicle septa. Black-grey scoriae show low vesicularity (< 25 vol.% in thin section), highly crystalline groundmass (glass < 30 vol.%), and abundant phenocrysts (PI up to 35%). Leucite, the most abundant phenocryst, is often characterized by crown-like poikilitic texture made up of clinopyroxene microcrysts (< 30 µm). Clinopyroxene is the second mineral in order of abundance and is present as *i*) submillimeter-sized, euhedral to subhedral, green- to deep-green-coloured phenocryst, similar to that occurring in white pumice, and *ii*) millimeter-sized, anhedral and colourless, phenocryst. The latter has been

interpreted as a xenocrystic population of clinopyroxene, on the basis of textural and chemical disequilibrium with the surrounding melt. The scarce sanidine is similar in shape as in white pumice. Plagioclase occurs either in glomerocrysts with clinopyroxene, or as microcrysts in the groundmass. Rare phenocrysts of biotite and apatite are also present. Notably, crystal-poor pumices and crystal-rich scoriae, although texturally different, share a similar bulk phonolitic composition (*e.g.*, Tufo Giallo della Via Tiberina eruptions; Masotta *et al.*, 2010).

#### Liquid line of descent and SVD plumbing system

Assuming the poorly differentiated phono-tephritic San Celso lava flow (Conticelli *et al.*, 1997) as possible parental composition in the SVD liquid line of descent, MELTS simulations indicates that at least 75 vol.% crystallization of the initial mass is required to obtain a phonolitic composition matching those of the yellow tuffs. However, such a large amount of crystals would have resulted in the production of differentiated melts locked into a non-eruptible crystal mush. Therefore, at least two stage of crystallization-differentiation (*i.e.*, two different depths) are required to produce the observed volumes of erupted phonolitic magma. This is in agreement with the whole compositions of natural products, showing a bimodal distribution of more and less differentiated products (Masotta *et al.*, 2012a) and, hence, with the inferred two-stage plumbing system (deep and primitive *vs.* shallow and differentiated; Fig. 1).

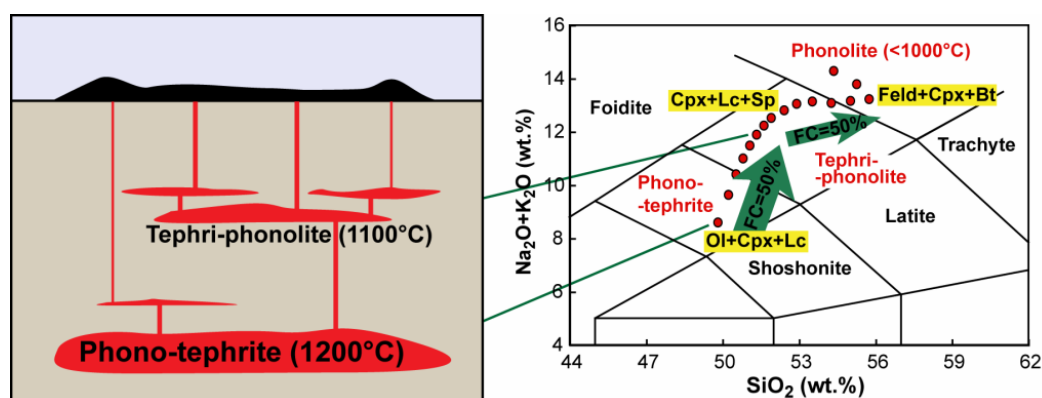


Fig. 1 - Sketch model of the SVD plumbing system as inferred from the overall composition of juvenile products and mass balance calculations obtained using MELTS code. Note that assuming a phono-tephritic primitive parental magma evolving toward phonolite, about 75% crystallization of initial mass would be required; this would freeze the system into a non-eruptible condition. Contrarily, a two-stage plumbing system would allow the differentiation of the phono-tephritic initial magma to produce and segregate an intermediate tephri-phonolitic magma that, in turn, differentiates at shallow crustal level producing phonolites.

#### Experimental evidences

Given the assumption of a shallow magma chamber feeding the explosive eruptions of SVD, phase equilibria and temperature gradient experiments used an intermediate tephri-phonolitic composition as starting material to constrain differentiation at low pressure. Hence, H<sub>2</sub>O-CO<sub>2</sub>-bearing phase equilibria experiments constrained the pre-eruptive conditions of the already differentiated phonolitic system.

#### Phase equilibria experiments

These experiments used as starting material a tephri-phonolitic scoria from Mt. Aguzzo scoria cone, emplaced during the activity of Sacrofano eruptive center (Sottili *et al.*, 2010). The charge was doped with *ca.* 2 wt.% of water and the experiments were performed at 300 MPa, in the temperature range 800-1100 °C for 24 hours. The runs performed at 1100 and 1050 °C produced only glass (super-liquidus condition). In the sub-liquidus runs, crystals were idiomorphic and homogeneous in distribution and size (10-12 μm). The crystal assemblage was made up of clinopyroxene, spinel, plagioclase, mica, sanidine, leucite, and amphibole. In runs

carried out at 1000 and 950 °C, clinopyroxene was the liquidus phase (1000 °C), it was ubiquitous at any investigated temperature, and formed diffuse clusters. Spinel occurred in scarce amount (< 1 vol.%) starting from 950 °C. Plagioclase appeared, simultaneously with mica, at 900 °C and became abundant at 850 °C forming large poikilitic crystal (> 100 µm) characterized by An-rich cores and Or-rich rims. At 800 °C the crystal fraction steeply increased as a consequence of multi-phase saturation of the liquid determining the crystallization of leucite and amphibole. At this temperature, the interstitial glass was scarce (as low as 13 vol.%) and feldspars prevailed over clinopyroxenes. The chemical composition of the interstitial glass varied as a function of temperature and degree of crystallization, spanning from tephri-phonolite (*i.e.*, starting material) to phonolite. In particular, interstitial melt became phonolitic in composition (comparable to SVD major eruptions products) at 900 °C and after ~ 30% crystallization. In the 850 °C run, the amount of glass decreased significantly (crystallinity ~ 50%).

#### Temperature gradient experiments

These experiments were performed in the temperature range 1050-850 °C taking advantage of the innate temperature gradient of graphite furnaces (Masotta *et al.*, 2012a), using the same starting material as in phase equilibria experiment and an initial water content of 2 wt.%. Phase relations and crystal fraction varied within the charges (from glassy to highly crystallized) according to the temperature gradient along the furnace. Crystalline phases were idiomorphic and, as in phase equilibria experiments, showed a constant size of 10-12 µm, with the exception of larger clinopyroxene and plagioclase (12-15 µm) in the near-liquidus region, and poikilitic feldspar (> 100 µm) and elongated sanidine (> 50 µm) in the low-temperature region. Notably, pockets and belts of (crystal-free) glass occurred at the top of the capsule, overlying a rigid framework of crystal, likely resembling a solidification front (*sensu* Marsh, 1996; Fig. 2). Melt chemical composition varied from the glassy zone at the bottom of the charge toward the highly crystallized zone. In particular, glass composition ranged from tephri-phonolite to phonolite in highly crystallized zone and in the large glassy pockets and belts.

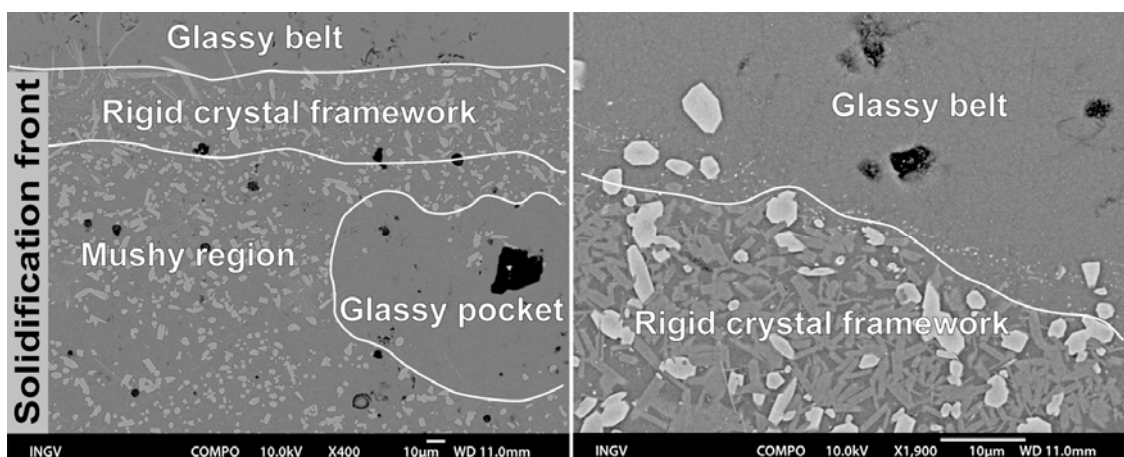


Fig. 2 - Details (backscattered images) of the cooler region (about 850 °C) of a temperature gradient experiment showing the glassy belts and pockets, the clinopyroxene+feldspar touching framework (rigid crystal framework) and the underlying crystal-rich portion (mushy region). This heterogeneously crystallized zone reproduces the theoretical 'solidification front' proposed by Marsh (1996).

#### H<sub>2</sub>O-CO<sub>2</sub>-bearing phase equilibria experiments

These experiments used a phonolitic pumice as starting material, doped with variable amounts of H<sub>2</sub>O and CO<sub>2</sub> (added as Ag<sub>2</sub>CO<sub>3</sub>). The runs were carried out at 200 MPa and in the temperature range of 850-950 °C. In agreement with natural products, clinopyroxene and feldspars dominate the mineral assemblage, being

ubiquitous in all the sub-liquidus runs and varying in proportions accordingly with temperature and volatiles concentration. Apparently, the presence of CO<sub>2</sub> did not affect significantly the stability of the mineral phases, although small variations in phase proportions were observed in experiments with similar conditions of T and X<sub>H<sub>2</sub>O</sub>, but different CO<sub>2</sub> concentration. Crystals were idiomorphic and ranged in size from 4 to 8 μm, hence being smaller and less homogeneous in size than those described in tephri-phonolite experiments. Clinopyroxene was roughly prismatic, whereas sanidine and plagioclase tend to form elongated crystals. Experiments carried out with H<sub>2</sub>O and CO<sub>2</sub> showed composition of the interstitial melt varying from phonolitic to trachytic, whereas in those performed adding only H<sub>2</sub>O, melt was always phonolitic in composition and slightly enriched in alkalis.

#### *Magma differentiation and solidification fronts*

Phase equilibria experiments constrained the role of clinopyroxene in driving melt differentiation and revealed that phonolitic interstitial glass was formed at temperature below 950 °C. The best matching between composition of glasses in experimental and natural products was, indeed, at 900 °C, with about 4 wt.% of H<sub>2</sub>O in the melt. At these conditions, although the composition of experimental phases matches that of natural ones, the highly crystallized texture of the experimental products set against the crystal-poor texture of natural ones. Actually, the isothermal environment reproduced by phase equilibria experiments might be not representative of the crystallization condition of shallow, thermally zoned magma chambers. To overcome this problem, temperature gradient experiment were designed with the aim of reproducing crystallization and differentiation in a thermally zoned environment. These experiments showed that differentiation varied as a function of crystallinity (in agreement with phase equilibria experiments) and, more importantly, that crystal-poor textures similar to those of natural products, could form at the cooler region of the capsule, where glassy (phonolitic) belts occurred over highly crystallized regions, representing the experimental analogue of a solidification front (Marsh, 1996).

In shallow, thermally zoned, magma chambers, the formation of a solidification front drove the differentiation process until the differentiated interstitial melt was extracted from the mush. Lithic enclaves erupted together with juvenile clasts during large eruptions witness the existence of a solidification front, but there was no record of the mechanisms leading to melt extraction. These mechanisms, indeed, could be explained only in light of experimental data from temperature gradient experiments.

#### *Crystal-melt separation in thermally-zoned magma chamber*

To explain the formation of glassy belts overlying the solidification fronts in temperature gradient experiments, at least three mechanism of crystal-melt separation can be considered: *i*) crystal settling, *ii*) compaction-induced segregation, and *iii*) collapse of the rigid crystal frame. Among these mechanisms, only the collapse of the rigid crystal frame is feasible. In fact, both the high viscosity of the system and the low contrast of densities between the solid and liquid phases would limit the efficacy of the settling process. Conversely, the hindering of crystals in the solidification front, forming the rigid crystal frame, would lead to the extrusion of the interstitial melt and consequent collapse of the crystal frame. Deformed sanidine crystals occurring at the interface between the glassy belt and the solidification front (Fig. 2) limit this process at a certain time of the experiment, after the formation of the solidification front (*i.e.*, when the interstitial melt is phonolitic in composition).

By analogy with evidences from temperature gradient experiments, the collapse of the rigid portions of the solidification front in a thermally zoned magma system may produce the extraction of the differentiated interstitial melt that in turn accumulates upward, forming the crystal-poor reservoir. Notably, in deposits associated to large explosive eruptions, the stratigraphic sequence of crystal-poor and crystal-rich products is reversed with respect to the position of crystal-poor and crystal-rich textures in the experimental charge. Moreover, the emplacement of primitive magmas during the post-caldera activity associated to these eruptions (feeding effusive activity) may be interpreted as the eruption of the deeper (hotter) and undifferentiated portion of the same magma system. Thus, considering a thermally zoned plumbing system analogue to that pictured by

experimental products, the stratigraphic relations among the erupted products could be related to a downward directed withdrawal mechanism (Spera, 1984; Blake & Ivey, 1986; Cioni *et al.*, 1995). In this scenario, crystal-poor products represent the top zone of the phonolitic magma chamber, being emplaced in the early phase of the eruption whilst crystal-rich products (fragments of the collapsed solidification front) are erupted in a later phase from an underlying crystal-rich zone (Fig. 3).

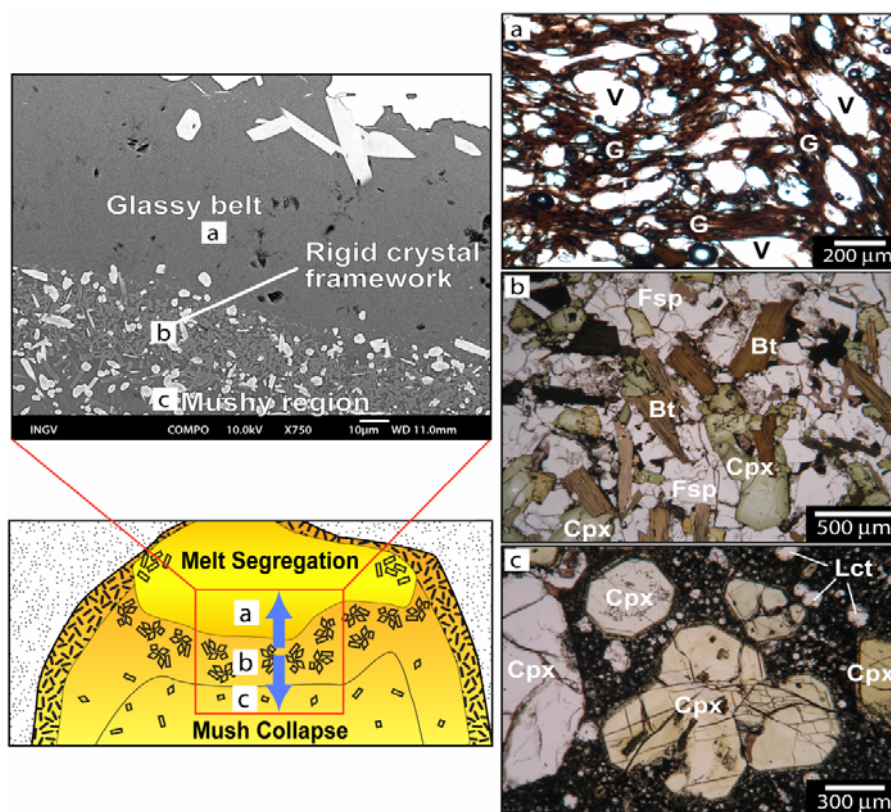


Fig. 3 - Comparison between textures of experimental and natural products of the SVD. a) The glassy belt at the top of the charge corresponds to natural crystal-poor juvenile clasts and represents the eruptible crystal-poor magma at the top of the magma chamber; b) the rigid crystal framework, and c) the mushy region correspond to crystal-rich products representing the collapsing portion of the solidification front. V: vesicles, G: glass, Fsp: feldspar, Cpx: clinopyroxene, Bt: biotite, Lct: leucite.

#### *H<sub>2</sub>O- and temperature-zoning of SVD magma system*

Temperature gradient experiments demonstrated that crystal-poor, differentiated melt accumulated at the roof of thermally zoned system, forming reservoirs of differentiated melt. The same mechanism might produce the crystal-poor reservoirs of differentiated magma feeding large explosive eruptions. Once these reservoirs were formed, magmatic differentiation continued and white pumice and black grey scoria magmas formed in response to thermal gradient. Phase equilibria experiments, coupled with MELTS simulations (Ghiorso & Sack, 1995) and cpx-liquid geothermometry (Putirka, 2008) were used to constrain pre-eruptive conditions of the “Tufo Giallo della Via Tiberina” eruptions, taken as case study for large caldera forming eruptions. Comparison between experimental and numerical results indicated that white pumice magma was erupted from a hotter zone (920-940 °C) than black-grey scoriae one (890-920 °C).

Temperature and H<sub>2</sub>O-zoning could be the factors controlling the degree of crystallization and phase relationships in different portions of magma chambers. Specifically, the presence of abundant lithic enclaves associated with black-grey scoria, suggests the tapping of different regions of the phonolitic reservoir during the

emission of white pumice and black-grey scoria in the course of individual eruptive event. Phase relationships and crystal growth rates data indicate that crystallization of relatively large leucite ( $> 100 \mu\text{m}$ ) should occur under  $\text{H}_2\text{O}$ -undersaturated conditions (Freda *et al.*, 2008; Shea *et al.*, 2009). Thus, the phonolitic black-grey scoria magma from the cooler and peripheral regions of the magma chambers was initially  $\text{H}_2\text{O}$ -undersaturated, allowing crystallization of leucite phenocrysts. Conversely, the lack of leucite phenocrysts in white pumice magma indicates a higher  $\text{H}_2\text{O}$  concentration and higher crystallization temperature. Moreover, the presence of round-shaped, partially resorbed, sanidine phenocrysts indicates that  $\text{H}_2\text{O}$ -saturation was achieved in the white pumice magma following feldspar crystallization. Given all these data, it has been deduced that extensive magma crystallization and consequent increase of  $\text{H}_2\text{O}$  at the periphery of the magma chamber (*i.e.*, the black-grey scoria feeder magma), produced  $\text{H}_2\text{O}$  migration toward the inner portion of the reservoir, where the higher temperature and increasing  $\text{H}_2\text{O}$  content acted to delay crystallization in the white pumice feeder magma. Once that the  $\text{H}_2\text{O}$  concentration gradient was established between the crystallizing peripheral regions of the magma chamber and the poorly crystallized inner portion, the  $\text{H}_2\text{O}$  mass flux was actually enhanced by the geometry of the magma system. Hence, considering a roughly concentric geometry of  $\text{H}_2\text{O}$ - and thermal zoning for the magma chamber, at each given point along the radial  $\text{H}_2\text{O}$ -gradient the mass of inward-migrating water would diffuse toward increasingly small volumes, so that the amount of dissolved water in the inner part of magma chamber would increase constantly, eventually leading to pre-eruptive  $\text{H}_2\text{O}$ -saturation. In this regard, re-melting features (*i.e.*, rounded-shape and glass-embayment) in sanidine from white pumice provide evidence of gradually increasing  $\text{H}_2\text{O}$  content that reduced the feldspars + leucite stability field in the inner portion of the magma chamber. Such a mechanism of  $\text{H}_2\text{O}$  migration toward the hottest region of the magma chamber is in agreement with experimental evidences of temperature gradient experiments. Indeed,  $\text{H}_2\text{O}$  concentration in the hotter, glassy region at the bottom of the charge was constantly increased, due to water diffusion from crystallizing zones. Thus, at the end of the experiments, the water concentration along the charge was actually constant.

The  $\text{H}_2\text{O}$ -saturation triggered the eruption of the white pumice magma in the hotter zone of the magma chamber. The decompression-induced crystallization of black grey scoria produced the fragmentation of the black grey scoria magma and its consequent eruption.

## CONCLUSION

Large explosive eruptions are typical of the activity of Sabatini Volcanic District. These eruptions produced texturally zoned deposits, characterized by abundant crystal-poor juvenile clasts at the bottom of the stratigraphic sequences and by crystal-rich ones at the top.

In order to explain such features, juvenile clasts representative of these deposits were collected and analyzed. Then, the experimental petrology allowed constraining the magmatic differentiation and the pre-eruptive conditions of the SVD magmatic system, as well as the crystal-melt separation processes leading to the origin of crystal-poor differentiated magmas. The results obtained from this study can be summarized as follows:

1) Differentiated magmas feeding large explosive eruptions of SVD are essentially phonolites plus rarer trachytes; less differentiated products, mostly phono-tephritic in composition, are commonly erupted during the post-caldera activity; intermediate compositions between phono-tephrites and phonolites are poorly represented. This compositional gap in the liquid line of descent of SVD magmas is interpreted in the light of a two-stages (shallow *vs.* deep) plumbing system. In analogy with other volcanic systems worldwide, the shallow thermally zoned magma chamber feeds the large explosive eruptions of SVD.

2) Phase equilibria experiments have constrained the SVD liquid line of descent. In particular, the phonolitic composition of the interstitial melt matches that of natural differentiated products below  $950^\circ\text{C}$  after a minimum of 30 vol.% crystallization of an intermediate (tephri-phonolite) starting material.

3) Temperature gradient experiments have confirmed the liquid line of descent obtained by phase equilibria experiments and, moreover, they have demonstrated that phonolitic interstitial melt forms in a solidification front and is then upward extracted during the collapse of the rigid crystal framework.

4) The matching between natural and experimental textures, as well as the stratigraphic relations between crystal-poor and crystal-rich textures in both natural and experimental products, indicate the collapse of the solidification front as a suitable mechanism producing crystal-poor, differentiated magmas.

5) Pre-eruptive temperature estimates for the phonolitic magmas feeding large explosive eruptions range from 890 to 940 °C; H<sub>2</sub>O content in the crystal-poor magma reached values up to 4-5 wt.% (H<sub>2</sub>O-saturation conditions), consequently to diffusion from the cooler, crystal-rich magma.

## REFERENCES

- Blake, S. & Ivey, G.N. (1986): Density and viscosity gradients in zoned magma chambers, and their influence withdrawal dynamics. *J. Volcanol. Geotherm. Res.*, **30**, 201-230.
- Cioni, R., Sbrana, A., Bertagnini, A., Buonasorte, A., Landi, P., Rossi, U., Salvati, L. (1987): Tephrostratigraphic correlations in the Vulcini, Vico and Sabatini volcanic successions. *Per. Mineral.*, **56**, 137-155.
- Cioni, R., Civetta, L., Marianelli, P., Metrich, N., Santacroce, R., Sbrana, A. (1995): Compositional layering and syn-eruptive mixing of periodically refilled shallow magma chamber: the A.D. 79 Plinian eruption of Vesuvius. *J. Petrol.*, **36**, 739-776.
- Coticelli, S. & Peccerillo, A. (1992): Petrology and geochemistry of potassic and ultrapotassic volcanism in Central Italy: petrogenesis and inferences on the evolution of the mantle sources. *Lithos*, **28**, 221-240.
- Coticelli, S., Francalanci, L., Manetti, P., Cioni, R., Sbrana, A. (1997): Petrology and geochemistry of the ultrapotassic rocks from the Sabatini Volcanic District, central Italy: the role of evolutionary processes in the genesis of variably enriched alkaline magmas. *J. Volcanol. Geotherm. Res.*, **75**, 107-136.
- Cundari, A. (1979): Petrogenesis of Leucite-bearing lavas in the Roman volcanic region, Italy. The Sabatini Lavas. *Contrib. Mineral. Petrol.*, **70**, 9-21.
- De Rita, D., Funicello, R., Parotto, M. (1988): Carta geologica del Complesso vulcanico dei Colli Albani. Progetto Finalizzato Geodinamica, C.N.R., Roma.
- De Rita, D., Funicello, R., Corda, L., Sposato, A., Rossi, U. (1993): Volcanic units. In: "Note illustrative della carta Sabatini volcanic Complex", M. Di Filippo, Ed. *Quad. Ric. Sci.*, **114**, 33-79.
- Freda, C., Gaeta, M., Misiti, V., Mollo, S., Dolfi, D., Scarlato, P. (2008): Magma-carbonate interaction: an experimental study on ultrapotassic rocks from Alban Hills (Central Italy). *Lithos*, **101**, 397-415.
- Ghiorso, M.S. & Sack, R.O. (1995): Chemical mass transfer in magmatic processes IV. A revised and internally consistent thermodynamic model for the interpolation and extrapolation of liquid-solid equilibria in magmatic systems at elevated temperatures and pressures. *Contrib. Mineral. Petrol.*, **119**, 197-212.
- Karner, D.B., Marra, F., Renne, P.R. (2001): The history of the Monti Sabatini and Alban Hills volcanoes: groundwork for assessing volcanic-tectonic hazards for Rome. *J. Volcanol. Geotherm. Res.*, **107**, 185-21.
- Marsh, B.D. (1996): Solidification fronts and magmatic evolution. *Mineral. Mag.*, **60**, 5-40.
- Masotta, M., Gaeta, M., Gozzi, F., Marra, F., Palladino, D.M., Sottili, G. (2010): H<sub>2</sub>O- and temperature-zoning in magma chambers: the example of the Tufo Giallo della Via Tiberina eruptions (Sabatini Volcanic District, central Italy). *Lithos*, **118**, 119-130.
- Masotta, M., Freda, C., Gaeta, M. (2012a): Origin of crystal-poor, differentiated magmas: insights from thermal gradient experiments. *Contrib. Mineral. Petrol.*, **163**, 49-65.
- Masotta, M., Freda, C., Paul, T.A., Moore, G.M., Gaeta, M., Scarlato, P., Troll, V.R. (2012b): "Low pressure" (P ≥ 150 MPa) experiments in the piston cylinder apparatus. *Chem. Geol.*, under revision.
- Peccerillo, A. (2005): Plio-Quaternary Volcanism in Italy. Springer-Verlag, Berlin Heidelberg, 365 p.
- Putirka, K.D. (2008): Thermometers and barometers for volcanic systems. In: "Minerals, Inclusions, and Volcanic Processes", K.D. Putirka & F. Tepley, Eds. *Rev. Mineral. Geochem.*, **69**, 61-120.
- Shea, T., Larsen, J.F., Gurioli, L., Hammer, J.E., Houghton, B.F., Cioni, R. (2009): Leucite crystal: surviving witnesses of magmatic processes preceding the 79 AD eruption at Vesuvius, Italy. *Earth Planet. Sci. Lett.*, **281**, 88-98.
- Sottili, G., Palladino, D.M., Marra, F., Jicha, B., Karner, D.B., Renne, P. (2010): Geochronology of the most recent activity in the Sabatini Volcanic District, Roman Province, central Italy. *J. Volcanol. Geotherm. Res.*, **196**, 20-30.
- Sottili, G., Palladino, D.M., Gaeta, M., Masotta, M. (2012): Maar eruptions from ultrapotassic magmas of the Roman Province: examples from the Sabatini Volcanic District (central Italy). *Bull. Volcanol.*, **74**, 163-186.
- Spera, F.J. (1984): Some numerical experiments on the withdrawal of magma from crustal reservoirs. *J. Geophys. Res.*, **89**, 8222-8236.